RSC Advances

PAPER

View Article Online
View Journal | View Issue

Cite this: *RSC Adv.*, 2017, **7**, 14010

Upconversion luminescence of Sm^{2+} ions

Xiaohui Liu,[a] Tuerxun Aidilibike,[ab] Junjie Guo,[a] Yangyang Li,[a] Weihua Di[a] and Weiping Qin*[a]

Received 3rd January 2017
Accepted 17th February 2017

DOI: 10.1039/c7ra00071e

rsc.li/rsc-advances

Herein, we report the phenomenon of upconversion luminescence from Sm^{2+} ions, which demonstrates that changeable valence lanthanides can serve as ions for optical frequency transformation. Upon excitation with a 980 nm diode laser, the doped Sm^{2+} ions in the hybrid material $BaFCl_{0.5}Br_{0.5}$:1%Sm^{2+}–CaF_2:1%Yb^{3+} emit red upconversion fluorescence peaks at 631 nm, 644 nm, 665 nm, 689 nm, 704 nm, and 729 nm from the $^5D_{0,1} \rightarrow {}^7F_{0,1,2}$ transitions. By transient dynamic analysis, we attributed the excitation of Sm^{2+} ions to the cooperation energy transfer process, in which two excited Yb^{3+} ions simultaneously transfer their energy to one Sm^{2+} ion.

Introduction

Upconversion luminescence (UCL) refers to a nonlinear optical process in which the sequential absorption of two or more photons leads to the emission of light at a shorter wavelength than the excitation wavelength (anti-Stokes type emission). Since the 1960s, optical frequency upconversion (UC) has been developed as a luminescence technology. The most important evolution of UC focuses on visible (VIS) UCL including red, green, and blue.[1–6] Owing to their excellent spectroscopic properties, lanthanide (Ln)-doped UCL materials have gained significant attention in the fields of 3D displays, light-emitting devices, biomarkers, bioassays, solid lasers, light-emitting diodes (LEDs), NIR photocatalysis, and temperature sensors.[7–16] In general, trivalent lanthanide ions, such as Tm^{3+}, Er^{3+}, Tb^{3+}, and Ho^{3+}, usually act as activators in UC materials, and Yb^{3+} ions with a large absorption cross-section in the NIR region[17,18] act as popular sensitizers to increase optical absorption.[19,20] In the past few decades, researchers used trivalent lanthanides with stable valence states in various UCL materials, and to date, almost no reports have been found on UCL from a divalent lanthanide ion or a changeable valence lanthanide, except for the study reporting UCL in Tm^{2+} materials in 2006 by Hans U. Güdel *et al.*[21] However, changeable valence lanthanides may produce more abundant wavelengths beyond those from trivalent lanthanides.

As a popular changeable valence lanthanide ion, Sm^{2+} has been heavily studied in the past few decades due to its red downconversion (DC) luminescence as well as its ability in optical storage.[22–25] Sm^{2+} has a similar electronic structure to that of Eu^{3+} and emits mainly bright red fluorescence in a downconversion way. Since the persistent spectral hole burning (PSHB) based on Sm^{2+} ions was reported, Sm^{2+}-doped fluoride halide mixed crystals have been exhibiting fascinating potential application in ultrahigh density optical data storage.[26–28] However, Sm^{2+} ion has never been considered as an UCL ion working in the regime of NIR excitation because it cannot be excited by a NIR photon or sensitized by an excited Yb^{3+} ion. In principle, two-photon absorption can possibly lead to the UCL of Sm^{2+} ions. However, to date, this has not been achieved because of the low efficiency ($\eta = \sim 10^{-13}$) of two-photon absorption.[29] Compared with two-photon absorption, the cooperative energy transfer (CET) from a Yb^{3+}-dimer to another lanthanide ion is more efficient ($\eta = \sim 10^{-6}$).[30] CET is the physical process in which two identical excited ions simultaneously exhibit transitions and transfer energy to another ion. Cooperative transition, which is closely associated with clustered lanthanide ions in solid hosts, involves cooperative luminescence (CL), cooperative absorption (CA), and CET. Clusters of lanthanide ions, such as Yb^{3+}-dimers, can easily form in the alkaline-earth fluoride crystal AF_2 (A = Ca, Sr, and Ba), depending on the type of lanthanide ion and its doping concentrations.[31,32] In ref. 30, the Yb^{3+} emission is a featureless band peaking at 497 nm, whereas a much more complex band with at least five individual peaks centered at around 520 nm was observed in the materials mentioned in this study. Calcium fluoride consists of a simple cubic lattice of fluorine ions in which every other body center position is occupied by a Ca^{2+} ion. Yb^{3+} ions occupy the Ca^{2+} sites when they are introduced into the CaF_2 lattice. Cooperative sensitization based on Yb^{3+}-dimers can excite Sm^{2+} ions by bridging the energy gap between the ground state and excited state of Sm^{2+} ions, yet it has not been performed to date.

The main reason for this should be that it is a real challenge to prepare a material simultaneously containing Yb^{3+} and Sm^{2+} ions using the conventional solid state reduction reaction. Samarium is a lanthanide that usually takes on a trivalent state, and an intense reduction reaction is needed to change it from

[a]*State Key Laboratory on Integrated Optoelectronics, College of Electronic Science & Engineering, Jilin University, Changchun, Jilin 130012, China. E-mail: wpqin@jlu.edu.cn*

[b]*Yili Normal University, Electronic and Information Engineering, Yining, Xinjiang 835000, China*

the trivalent state to the divalent state. However, trivalent ytterbium has a similar reduction-oxidation potential as that of trivalent samarium; thus, it will also be reduced to the bivalent state under the same conditions for the reduction of trivalent samarium ions. Therefore, a reasonable synthetic route should be considered for the coexistence of Sm^{2+} ions and Yb^{3+} ions in a material.

Herein, we synthesized a hybrid material containing the Yb^{3+}-dimer and Sm^{2+} ions *via* a stepwise synthetic reaction and report the first experimental observation of UC emissions from Sm^{2+} ions upon 980 nm excitation.

Experimental

Yb^{3+}-doped CaF_2 and Sm^{2+}-doped $BaFCl_{0.5}Br_{0.5}$ were prepared *via* high temperature solid state reactions in argon and reducing atmospheres, respectively. Stoichiometric amounts of the raw materials CaF_2 and YbF_3 (1 mol%) were thoroughly mixed by grinding and heated to 1200 °C for 2 h in an Ar atmosphere. Sm^{3+}-doped $BaFCl_{0.5}Br_{0.5}$ was prepared in the same way but in a H_2 reducing atmosphere. A suitable melting temperature is the key to ensure a close enough distance between Yb^{3+} and Sm^{2+} ions and achieve efficient energy transfer from the Yb^{3+}-dimers to Sm^{2+} ions. To make this a reality, the prepared powders $BaFCl_{0.5}Br_{0.5}$:1%Sm^{2+} and CaF_2:1%Yb^{3+} were mixed in the mass ratio of 1 : 1 and annealed at 900 °C in an Ar atmosphere for 10 min to obtain the final hybrid material $BaFCl_{0.5}Br_{0.5}$:1%Sm^{2+}–CaF_2:1%Yb^{3+}.

Characterization

A Rigaku RU-200b X-ray powder diffractometer (XRD) was used to analyze the crystal structures using nickel-filtered Cu-Kα radiation ($\lambda = 0.15405$ nm) in the range of $10^\circ \leq 2\theta \leq 70^\circ$. The accelerating voltage was 40 kV, and the emission current was 200 mA. Absorption spectra in the UV to NIR region were obtained using a Shimadzu UV3600 spectrophotometer in the range of 200–1100 nm. Excitation and emission spectra were obtained using a Hitachi F-4500 spectrometer equipped with a Hamamatsu R928 photomultiplier (PMT) and a 2 W 980 nm continuous wave diode laser as the excitation source. Luminescence spectra were obtained using a one-meter monochromator (SPEX 1000M; HORIBA Jobin Yvon Inc., Edison, NJ, USA) equipped with an 1800 line mm^{-1} grating. The excitation light source was a power adjustable continuous wave laser diode (978 nm, 10 W; BWT Beijing Ltd, Beijing, China). Spectral measurements at low temperature were performed using a helium-cycled cryostat (ARS-2HW; Advanced Research Systems, Macungie, PA, USA). A digital oscilloscope (DPO4104B, bandwidth 1 GHz, sampling rate 5 GSs^{-1}; Tektronix, Shanghai, China), a power-adjustable continuous wave laser diode (CW978 nm, 10 W), and a chopper were used to obtain the decay curves.

Results and discussion

The composition and phase purity of the products were first examined by XRD. It is well known that CaF_2 has a cubic crystal structure and its lattice parameter values are $a = 5.463$ nm, $b = 5.463$ nm, and $c = 5.463$ nm. The blue line in Fig. 1a shows the XRD patterns of the as-prepared CaF_2:1%Yb^{3+}. All the patterns can be indexed to the pure cubic phase of CaF_2 (JCPDS 4-864) and no impurity peaks were observed. There is no standard card corresponding to the sample $BaFCl_{0.5}Br_{0.5}$:1%Sm^{2+} since it is a fluoride halide-mixed crystal (Fig. 1a, red line). According to the XRD patterns of the products, neither impurity peaks nor a second phase can be detected at the current mixing level. This clearly implies that the doping of Yb^{3+} and Sm^{2+} ions does not cause any significant change in the host structure.

The absorption spectra of obtained powder samples, with the characteristic bands of Sm^{2+} ions and Yb^{3+} ions in the UV-vis and the near-infrared (NIR) regions, respectively, reveal the existence of both Sm^{2+} and Yb^{3+} ions, as shown in Fig. 1b. The absorption band at around 950 nm is attributed to the electronic transition from the $^2F_{7/2}$ ground state to the $^2F_{5/2}$ excited states of Yb^{3+} ions. For the samples doped with Sm^{2+} ions, an obvious broad absorption band with four peaks (black and blue curves) appears in the UV-vis region, which are assigned to the 4f5d bands of Sm^{2+} ions. The emission spectrum of $BaFCl_{0.5}Br_{0.5}$:1%Sm^{2+}–CaF_2:1%Yb^{3+} was obtained under 408 nm excitation, which is shown as the black line in Fig. 1c. The emissions consist of several sharp peaks in the region from 600 to 750 nm, which are assigned to the $^5D_0 \rightarrow {}^7F_j$ ($j = 0$, 1, and 2) and $^5D_1 \rightarrow {}^7F_j$ ($j = 0$, 1, and 2) transitions of Sm^{2+} ions. It is well-known that the 689 nm emission from the $^5D_0 \rightarrow {}^7F_0$ transition of Sm^{2+} ions is efficient and well isolated. To understand the origin of the emissions, the excitation spectra of the 4f5d bands were obtained by monitoring the transition of $^5D_0 \rightarrow {}^7F_0$ (689 nm), as shown in Fig. 1d. It can be seen that there are four main peaks in the 4f5d band. The half diffraction peak of the emission $^5D_0 \rightarrow {}^7F_0$ is located at about 345 nm. The UC emissions of $BaFCl_{0.5}Br_{0.5}$:1%Sm^{2+}–CaF_2:1%Yb^{3+} was obtained under 978 nm excitation, which is shown as the red line in Fig. 1c. The emission curve is almost the same as that in the DC spectrum of $BaFCl_{0.5}Br_{0.5}$:1%Sm^{2+} without Yb^{3+} ions, indicating that two different ways of excitation can induce the emissions of Sm^{2+} ions. Therefore, it is reasonable to attribute the UC emission peaks at 631 nm, 644 nm, 665 nm, 689 nm, 704 nm, and 729 nm to the ^5D_i ($i = 0$, 1) $\rightarrow {}^7F_j$ ($j = 0$, 1, 2) transitions of the Sm^{2+} ion.

Under the pumping of an NIR laser, a pair of Yb^{3+} ions (Yb^{3+}-dimer) were both exited from the $^2F_{7/2}$ to $^2F_{5/2}$ level, and then depopulated from the excited state $^2F_{5/2}$ simultaneously to emit a visible photon, which is called cooperative luminescence. Fig. 2a shows the photoluminescence spectrum of the mixture, hybrid, and CaF_2:1%Yb^{3+} under 980 nm excitation. A broad band ranging from 470 to 570 nm is observed, which originates from the cooperative luminescence of the Yb^{3+}-dimers. It was found that this broad band is composed of a few sharp emission peaks connected with each other. It is well-known that the $^2F_{5/2}$ to $^2F_{7/2}$ levels of Yb^{3+} ions split into three and four Stark components in a tetragonal crystal field, respectively.[33] Therefore, a random combination of two Stark components in the cooperative luminescence of a Yb^{3+}-dimer forms emissions located at different energies but close to each other.[34] These approaching emission peaks are connected to form a broad band.

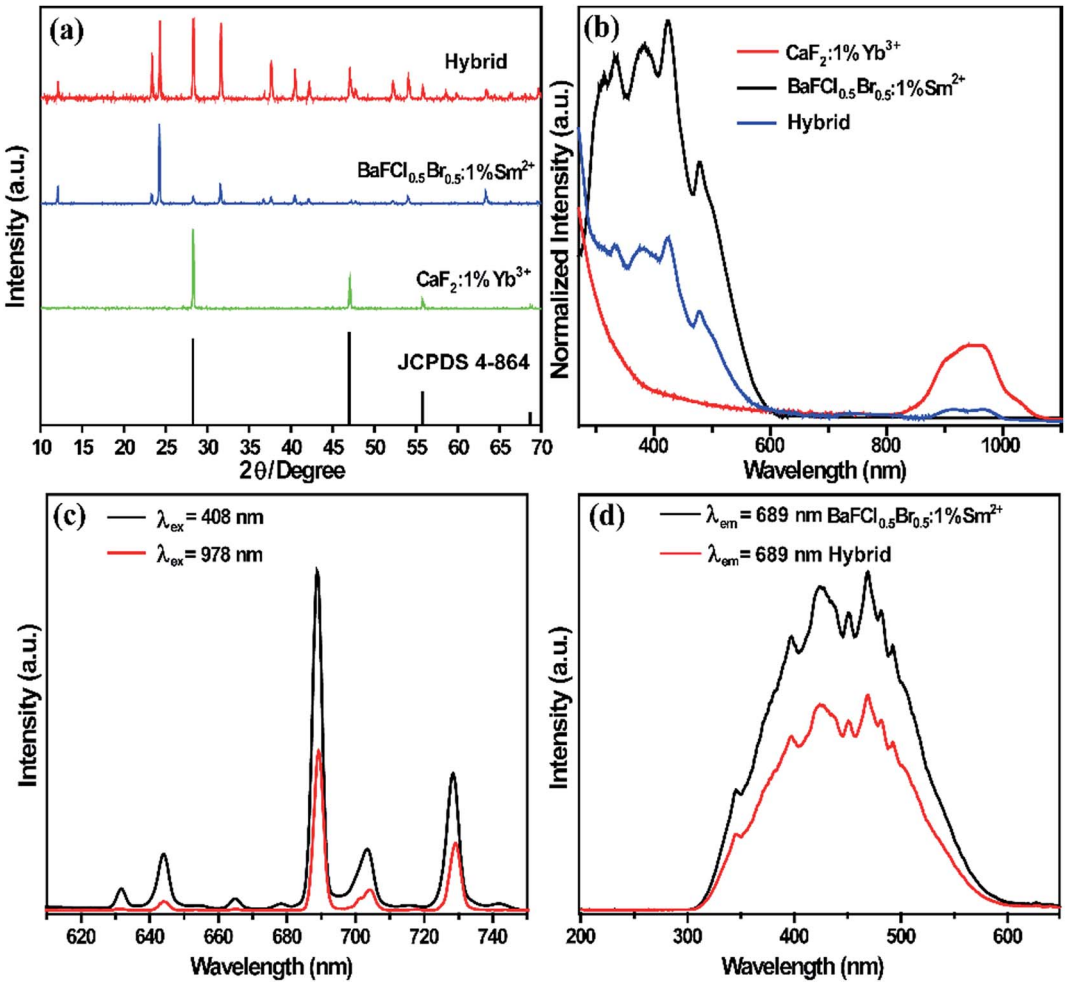

Fig. 1 (a) XRD patterns of $BaFCl_{0.5}Br_{0.5}$:1%Sm^{2+}–CaF_2:1%Yb^{3+} (hybrid), $BaFCl_{0.5}Br_{0.5}$:1%Sm^{2+} and CaF_2:1%Yb^{3+}. (b) Absorption spectra of the obtained samples. (c) Emission spectrum of $BaFCl_{0.5}Br_{0.5}$:Sm^{2+} upon 408 nm excitation, and UC spectrum of Sm^{2+} in the hybrid material under 978 nm excitation. (d) Photoluminescence excitation spectra of hybrid and $BaFCl_{0.5}Br_{0.5}$:1%Sm^{2+} by monitoring the emission of Sm^{2+} ions at 689 nm.

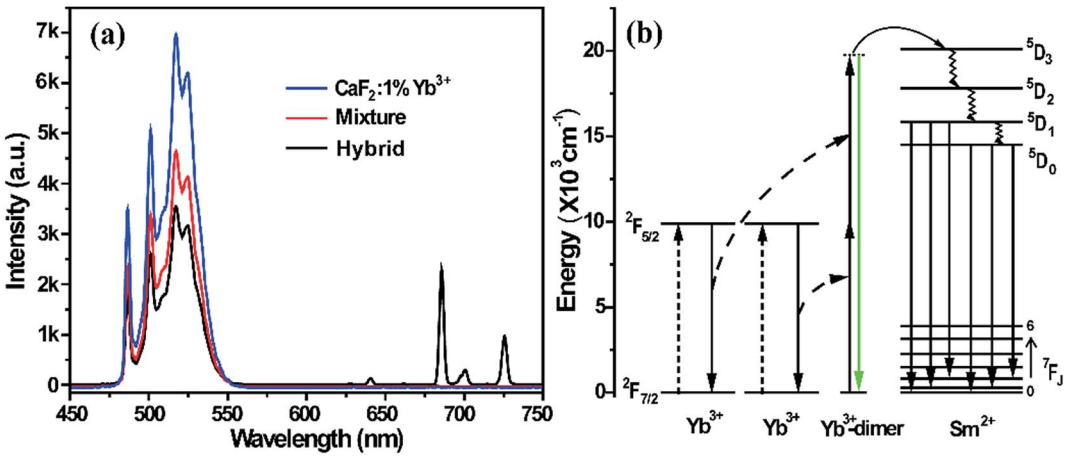

Fig. 2 (a) Emission spectra (450–750 nm) of the hybrid, CaF_2:1% Yb^{3+} and mixture materials upon 978 nm excitation at room temperature. (b) Schematic for the energy level diagram of Yb^{3+} and Sm^{2+} ions and possible UC population and emission processes.

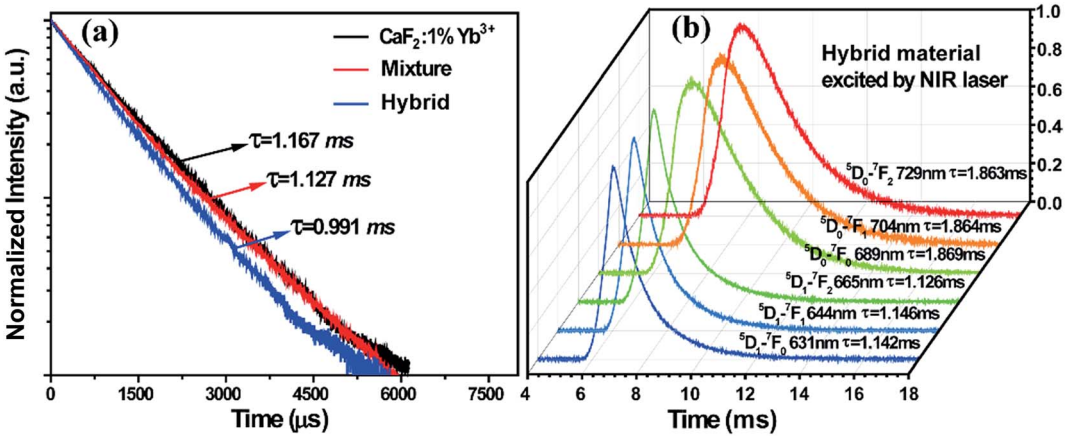

Fig. 3 (a) Decay curves of cooperative luminescence from Yb^{3+}-dimers by monitoring the 500 nm emission of $BaFCl_{0.5}Br_{0.5}$:1%Sm^{2+}–CaF_2:1% Yb^{3+}, CaF_2:1%Yb^{3+} and the mixture under 978 nm excitation. (b) UC photoluminescence decay curves of the $^5D_i \rightarrow {}^7F_j$ transitions of Sm^{2+} ions at room temperature.

As shown in Fig. 2a and 1d, there is obvious spectral overlap between the emission of the Yb^{3+}-dimers and the excitation of Sm^{2+} ions. Radiation reabsorption may happen when the excitation and emission spectra overlap. However, there is no UCL in the physical mixture of $BaFCl_{0.5}Br_{0.5}$:1%Sm^{2+} and CaF_2:1% Yb^{3+}, which indicates that the mechanism of radiation reabsorption does not play a main role in the process of UCL of Sm^{2+} ions. In contrast, the emissions of Yb^{3+}-dimers are still very strong in the hybrid material, and Yb^{3+}-dimers have a partial radiative transition accompanied with CL, thus demonstrating that only some of the energy of the Yb^{3+}-dimers transfers to Sm^{2+} ions and realizes the UCL of Sm^{2+} ions. Fig. 2b schematically describes the possible UC processes in the energy level diagrams of the cooperation energy transfer from Yb^{3+} to Sm^{2+} ions. The large energy gap between the ground state and the excited state in Sm^{2+} ions requires the cooperation sensitization of Yb^{3+}-dimers because there is no intermediate level in Sm^{2+} that can be resonant with a 980 nm photon or an excited Yb^{3+} ion. Under the NIR laser excitation, an Yb^{3+}-dimer simultaneously absorbs two NIR photons and then transfers their energy to a Sm^{2+} ion through a cooperative sensitization process to promote it to the state of $^5D_3$. The lower energy levels $^5D_{0,1}$ can be populated through a series of non-radiative relaxations from the higher $^5D_3$ state.

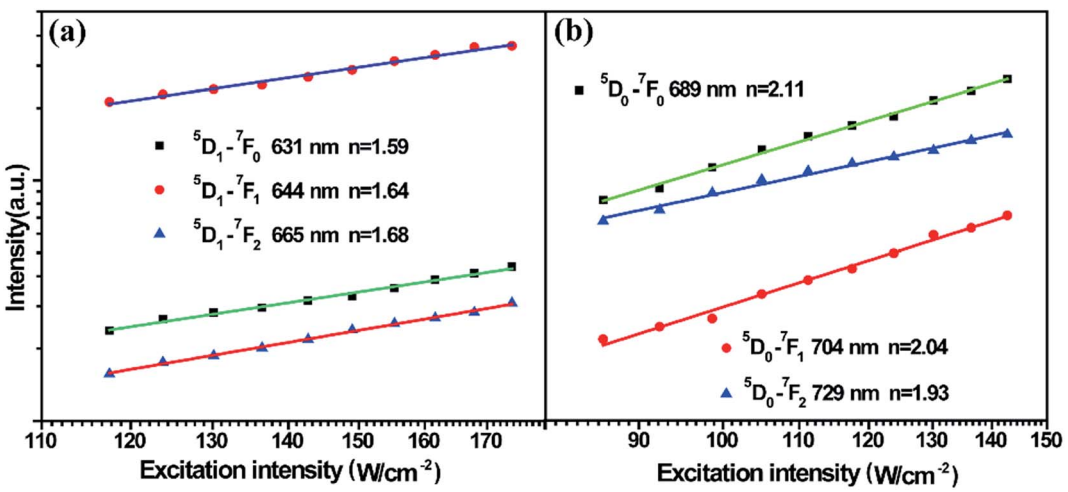

Fig. 4 (a) Excitation power dependence of the UCL of $^5D_1 \rightarrow {}^7F_j$ ($j = 0, 1, 2$) in Sm^{2+} ions. (b) Excitation power dependence of UCL of $^5D_0 \rightarrow {}^7F_j$ ($j = 0, 1, 2$) in Sm^{2+} ions.

Table 1 The photon number n with different transitions

Emitting level	$^5D_1 \rightarrow {}^7F_0$	$^5D_1 \rightarrow {}^7F_1$	$^5D_1 \rightarrow {}^7F_2$	$^5D_0 \rightarrow {}^7F_0$	$^5D_0 \rightarrow {}^7F_1$	$^5D_0 \rightarrow {}^7F_2$
Number of photons	1.59	1.64	1.68	2.11	2.04	1.93

To further confirm the CET from the Yb^{3+}-dimers to Sm^{2+} ions, the excited state dynamics was investigated under 978 nm excitation by monitoring the emission of Yb^{3+}-dimers at 500 nm, as shown in Fig. 3a. The decay time of the Yb^{3+}-dimers decreases in the hybrid material, indicating that CET occurred between the Yb^{3+}-dimers and Sm^{2+} ions. It can be seen that these decay curves have no rising edge, which means that the CL of the Yb^{3+}-dimers originates from the direct excitation of 978 nm and no energy transfer process exists. However, the UCL of Sm^{2+} ions shows a rising edge, as shown in Fig. 3b, which indicates that the energy that stimulates Sm^{2+} ions originates from the energy transfer of the Yb^{3+}-dimers. The decay times were measured at around 1.13 ms and 1.86 ms for the $^5D_1 \rightarrow {}^7F_{0,1,2}$ and $^5D_0 \rightarrow {}^7F_{0,1,2}$ transitions of Sm^{2+} ions, respectively. The decay parts of these curves can be fitted well into a single-exponential function as $I = I_0 \exp(-t/\tau)$ (I_0 is the initial emission intensity at $t = 0$, and τ is the lifetime), demonstrating the populating processes as discussed above.

To fully analyse the nature of the UC processes, the dependence of the integral luminescence intensities on the pumping laser power (at 978 nm) was examined. For an unsaturated UC process, the integrated UCL intensity I_f is proportional to P^n, where, P denotes the pumping power, and the exponent n represents the number of photons involved in populating the upper emitting state in the UC process. Fig. 4 shows the typical double-logarithmic plots of UCL intensities *versus* the pump power densities. The values of the photon number n are listed in Table 1. It can be seen from the table that these transitions are of two-photon UC processes. This result corresponds to the analysis of the UC population and emission processes in the schematic energy level diagram of the Sm^{2+} ion and Yb^{3+}-dimer.

Conclusion

In summary, the hybrid phosphor $BaFCl_{0.5}Br_{0.5}$:1%Sm^{2+}–CaF_2:1%Yb^{3+} was prepared *via* a stepwise high temperature reaction to achieve a material containing both Yb^{3+} and Sm^{2+} ions. The UCL of the ^5D_i ($i = 0, 1$) $\rightarrow {}^7F_j$ ($j = 0, 1, 2$) transitions from Sm^{2+} was observed under NIR excitation. The analysis results indicate that the population of Sm^{2+} excited states originates from the cooperative energy transfer of Yb^{3+}-dimers. Based on our results, it is actually possible to achieve the upconversion luminescence of changeable valence lanthanides under NIR excitation, which moreover, opens up a new field for the upconversion of rare earth ions.

Acknowledgements

This work was supported by the National Natural Science Foundation of China (NSFC) (Grants 11474132 and 11274139).

Notes and references

1 L. Johnson and H. Guggenheim, *Appl. Phys. Lett.*, 1973, **23**, 96–98.
2 A. Silversmith, W. Lenth and R. Macfarlane, *Appl. Phys. Lett.*, 1987, **51**, 1977–1979.
3 R. Macfarlane, F. Tong, A. Silversmith and W. Lenth, *Appl. Phys. Lett.*, 1988, **52**, 1300–1302.
4 T. Danger, J. Koetke, R. Brede, E. Heumann, G. Huber and B. Chai, *J. Appl. Phys.*, 1994, **76**, 1413–1422.
5 M.-F. Joubert, *Opt. Mater.*, 1999, **11**, 181–203.
6 M. Pollnau, D. Gamelin, S. Lüthi, H. Güdel and M. Hehlen, *Phys. Rev. B: Condens. Matter Mater. Phys.*, 2000, **61**, 3337.
7 W. Miniscalco, L. Andrews, B. Thompson, R. Quimby, L. Vacha and M. Drexhage, *Electron. Lett.*, 1988, **24**, 28–29.
8 J. Allain, M. Monerie and H. Poignant, *Electron. Lett.*, 1991, **27**, 1156–1157.
9 J. Allain, M. Monerie and H. Poignant, *Electron. Lett.*, 1992, **28**, 111–113.
10 H. Többen, *Electron. Lett.*, 1992, **28**, 1361–1362.
11 W. Park, M. Jung and D. Yoon, *Sens. Actuators, B*, 2007, **126**, 324–327.
12 L. Yi, X. He, L. Zhou, F. Gong, R. Wang and J. Sun, *J. Lumin.*, 2010, **130**, 1113–1117.
13 J. Alonso, J. Ferrer, A. Salinas-Castillo, R. Mallavia and S. F. de Ávila, *Solid-State Electron.*, 2010, **54**, 1269–1272.
14 W. Qin, D. Zhang, D. Zhao, L. Wang and K. Zheng, *Chem. Commun.*, 2010, **46**, 2304–2306.
15 L. Wei, S. Doughan, Y. Han, M. V. DaCosta, U. J. Krull and D. Ho, *Sensors*, 2014, **14**, 16829–16855.
16 Y. Tang, W. Di, X. Zhai, R. Yang and W. Qin, *ACS Catal.*, 2013, **3**, 405–412.
17 J. Nees, S. Biswas, F. Droun, J. Faure, M. Nantel, G. A. Mourou, A. Nishimura, H. Takuma, J. Itatani and J.-C. Chanteloup, *IEEE J. Sel. Top. Quantum Electron.*, 1998, **4**, 376–384.
18 A. Diening, P.-A. Möbert and G. Huber, *J. Appl. Phys.*, 1998, **84**, 5900–5904.
19 D. Dosev, I. Kennedy, M. Godlewski, I. Gryczynski, K. Tomsia and E. Goldys, *Appl. Phys. Lett.*, 2006, **88**, 1906.
20 S. Das, A. A. Reddy and G. V. Prakash, *Chem. Phys. Lett.*, 2011, **504**, 206–210.
21 E. Beurer, J. Grimm, P. Gerner and H. U. Güdel, *J. Am. Chem. Soc.*, 2006, **128**(10), 3110–3111.
22 W. Kaiser, C. Garrett and D. Wood, *Phys. Rev.*, 1961, **123**, 766.
23 J. O'Connor and H. Bostick, *J. Appl. Phys.*, 1962, **33**, 1868–1870.
24 G. H. Dieke and R. Sarup, *J. Chem. Phys.*, 1962, **36**, 371–377.
25 D. Wood and W. Kaiser, *Phys. Rev.*, 1962, **126**, 2079.
26 R. Jaaniso and H. Bill, *Europhys. Lett.*, 1991, **16**, 569.
27 K. Holliday, C. Wei, M. Croci and U. P. Wild, *J. Lumin.*, 1992, **53**, 227–230.
28 J. Zhang, S. Huang, W. Qin, D. Gao and J. Yu, *J. Lumin.*, 1992, **53**, 275–278.
29 E. Bayer and G. Schaack, *Phys. Status Solidi B*, 1970, **41**, 827–835.
30 T. Kushida, *J. Phys. Soc. Jpn.*, 1973, **34**, 1327–1333.
31 E. Nakazawa and S. Shionoya, *Phys. Rev. Lett.*, 1970, **25**, 1710.
32 V. Petit, P. Camy, J.-L. Doualan, X. Portier and R. Moncorgé, *Phys. Rev. B: Condens. Matter Mater. Phys.*, 2008, **78**, 085131.
33 M. J. Weber and R. W. Bierig, *Phys. Rev. B: Condens. Matter Mater. Phys.*, 1964, **134**, A1492.
34 W. P. Qin, Z. Y. Liu, C. N. Sin, C. F. Wu, G. S. Qin, Z. Chen and K. Z. Zheng, *Light: Sci. Appl.*, 2014, **3**, e193.

